HHS Public Access

Author manuscript

Nature. Author manuscript; available in PMC 2010 September 04.

Published in final edited form as:

Nature. 2010 March 4; 464(7285): 104–107. doi:10.1038/nature08780.

Circulating Mitochondrial DAMPs Cause Inflammatory Responses to Injury

Qin Zhang, **Mustafa Raoof**, **Yu Chen**, **Yuka Sumi**, **Tolga Sursal**, **Wolfgang Junger**, **Karim Brohi**[*], **Kiyoshi Itagaki**, and **Carl J. Hauser**

Department of Surgery, Division of Trauma, Beth Israel Deaconess Medical Center and Harvard Medical School, Boston MA 02215 USA

[*] Queen Mary University of London

Abstract

Injury causes a systemic inflammatory response syndrome (SIRS) clinically much like sepsis 1. Microbial pathogen-associated molecular patterns (PAMPs) activate innate immunocytes through pattern recognition receptors 2. Similarly, cellular injury can release endogenous damage-associated molecular patterns (DAMPs) that activate innate immunity 3. Mitochondria are evolutionary endosymbionts that were derived from bacteria 4 and so might bear bacterial molecular motifs. We show here that injury releases mitochondrial DAMPs (MTD) into the circulation with functionally important immune consequences. MTD include formyl peptides and mitochondrial DNA. These activate human neutrophils (PMN) through formyl peptide receptor-1 and TLR9 respectively. MTD promote PMN Ca^{2+} flux and phosphorylation of MAP kinases, thus leading to PMN migration and degranulation *in vitro* and *in vivo*. Circulating MTD can elicit neutrophil-mediated organ injury. Cellular disruption by trauma releases mitochondrial DAMPs with evolutionarily conserved similarities to bacterial PAMPs into the circulation. These can then signal through identical innate immune pathways to create a sepsis-like state. The release of such mitochondrial ‘enemies within’ by cellular injury is a key link between trauma, inflammation and SIRS.

Trauma is a leading cause of premature death 5. Injury causes activation of neutrophils (PMN), organ failure, susceptibility to infection and the Systemic Inflammatory Response Syndrome (SIRS) 1,6. Bacterial translocation from ischemic gut to circulation was long thought to cause SIRS 7. This was disproven 8 although shock may cause gut inflammation 9. Crushes and burns however, cause SIRS without shock. Thus the molecular signals linking injury to inflammation remain unclear.

Correspondence and requests for materials should be addressed to C.J.H (cjhauser@bidmc.harvard.edu).

Author Information Reprints and permissions information is available at npg.nature.com/reprintsandpermissions.

Supplementary Information is linked to the online version of the paper at www.nature.com/nature

Author Contributions Experiments were conceived and designed by CJH, QZ, KI and WJ. Experiments were performed by QZ, MR, YC, YS, WJ, KB and TS. Data were analyzed by QZ and CJH. The paper was written by QZ, MR and CJH.

During infection, innate immunity is activated by pathogen-associated molecular patterns (PAMPs) expressed on invading microorganisms. Pattern recognition receptors (PRR) recognize PAMPs 2. Bacterial proteins are *N*-formylated 10, so formyl peptides (FP) activate chemoattractant FP-receptors (FPR). Toll-like receptors (TLR) respond to many PAMPs, like bacterial DNA that stimulates TLR9. Since mitochondria evolved from saprophytic bacteria to endosymbionts to organelles, the mitochondrial genome (mtDNA) contains CpG DNA repeats and also codes for formylated peptides 4,11. Mechanical trauma disrupts cells, so we hypothesized injury might release mitochondrial "damage" associated molecular patterns (DAMPs) 3 into the circulation, activating immunity and initiating SIRS.

To prove trauma releases mitochondrial DAMPs (MTD) into the circulation we measured plasma mtDNA in 15 major trauma patients (Injury Severity Score [ISS 12] >25). Sampling was prior to resuscitation. Patients had no open wounds or gastrointestinal injuries (Details: Supplementary Table 1). Trauma patient mtDNA was markedly elevated (Supplementary Figs. 1a–c) compared to volunteers (Supplementary Table 2). mtDNA in trauma plasma was 2.7±0.94[SE] μg/ml where volunteer levels were thousands of fold lower (Supplementary Fig. 1d). mtDNA was further elevated 24hrs post-injury (Supplementary Fig. 1e). Ultra-centrifugates of femur reaming specimens obtained during fracture repair contained even higher titers of mtDNA. Thus MTD are mobilized by external or operative injury and enter the circulation. Bacterial 16s-RNA was absent from all specimens (Supplementary Fig. 1f).

Mitochondrial formyl peptides (FP) can attract PMN 13 and activate related cell lines 14. The synthetic peptide fMLF simulates bacterial challenge. But the role of endogenous formyl peptides in trauma, PMN activation and SIRS is unstudied. FPs signal via the G-protein coupled receptors (GPCR); FPR1 and FPRL-1, with high and low affinities respectively. PMN activation via GPCR causes increased intracellular calcium ($[Ca^{2+}]_i$) 15, heterologous and homologous GPCR desensitization 16 and activates MAP Kinases 17. MTD from human myocytes induced human PMN $[Ca^{2+}]_i$ fluxes equal to 1nM fMLF (Fig. 1a). MTD from human liver, muscle and fracture hematoma (Supplementary Fig. 2a) or from rat muscle or liver produced similar PMN Ca^{2+} depletion. Whole and fragmented mitochondria had similar potency (Supplementary Fig. 2b). Thus release of MTD from many cell types activates immunity.

Blocking antibodies to FPR1 abolished Ca^{2+} depletion (Fig. 1a), and Ca^{2+} entry (Fig. 1b) responses to MTD. Cyclosporin H (CsH) inhibits FPR118 and abolishes Ca^{2+} flux to MTD (Supplementary Fig. 3a). Isotype control (FPRL-1, MMP-2) antibodies have no effects (Supplementary Fig. 3b). Apyrase-treated and untreated MTD act identical whereas apyrase abolishes $[Ca^{2+}]_i$ response to ATP (Supplementary Fig. 3c). ATP was undetectable on random assays of MTD (n=3).

Activating FPR1 desensitizes chemokine receptors, predisposing to infection after trauma 16. Human PMN treated with MTD became insensitive to GRO-α (CXCL1, Fig. 1c). PMN stimulated by GRO-α, MTD or buffer (Fig. 1d) show identical Ca^{2+} release by ionomycin. Since Ca^{2+} stores are equal, suppression by MTD reflects CXCR2 desensitization by FPR1. PMN also show homologous desensitization when re-challenged with MTD (Fig. 1e) or fMLF (Supplementary Fig. 4). Others have shown that PMN MAP kinases are

phosphorylated and activated by injury 17. Skeletal muscle MTD caused phosphorylation of PMN p38 and p44/42 MAP kinases (Fig. 2a and 2b) with p38 being activated at lower concentrations. Thus muscular injury can liberate mitochondrial DAMPs that activate multiple inflammatory signal pathways.

Mitochondrial DAMPs activate PMN signaling, so next we studied whether they elicit an inflammatory PMN phenotype. Matrix metalloproteinase (MMP)-8 is a neutrophil-specific collagenase 19 that aids in PMN tissue penetration and recruitment. Interleukin (IL)-8 causes PMN chemotaxis and activation, and such PMN activation also induces secondary IL-8 release. MTD caused MMP-8 release from human PMN (Fig. 2c). Inhibition by CsH or anti-FPR1 demonstrates FPR1-dependence (Fig. 2d). Human PMN synthesized and released IL-8 in response to MTD (Fig. 2e/f) more rapidly than to LPS. This “bell-shaped” response curve (Fig. 2e) may reflect FPR1 suppression by high concentrations of MTD (see Fig. 1e). In longer incubation studies, LPS was more potent (Fig. 2f).

PMN use lytic enzymes like MMPs to migrate into bystander organs. We assessed the effects of MTD on PMN migration. Under video-microscopy PMN migrated toward MTD from clinical femur fractures (Figures 2g–j, supplementary videos 1–4). Speed and directionality of migration were inhibited by CsH 18 (Fig 2i, Video 3) or by antibodies to FPR1 (Fig 2j, Video 4). Last, we showed *in vivo* PMN infiltration in response to clinical concentrations of MTD by placing enough liver-derived MTD into mouse peritoneum to model traumatic necrosis of 10% of the mouse’s liver. Neutrophilic peritonitis developed quickly (Fig. 2k). MTD was more active than the FPR agonist W-peptide and CsH again reduced peritonitis (Fig. 2k).

Mitochondria contain their own genome, but mtDNA resembles bacterial DNA in being circular and having nonmethylated CpG motifs 20. mtDNA has been found in joint fluids in rheumatoid arthritis and induces inflammation *in vivo* 21. CpG DNA activates TLR9 but activation of PMN by mtDNA is unstudied. TLR9 is expressed by PMN 22 and activates p38 MAPK 23. So we questioned whether PMN p38 MAPK would be activated by mtDNA at clinical plasma concentrations (Supplementary Fig. 1d). We found 1μg/ml mtDNA caused p38 MAPK phosphorylation (Fig. 3a) but did not activate p44/42 MAPK. p38 MAPK activation was blocked by inhibitory oligodeoxynucleotides (ODN TTAGGG, Fig. 3b) that bind CpG motifs and block interactions with TLR9. Looking at downstream signaling, we incubated PMN with CpG DNA (10μg/ml) or mtDNA within the clinical range (1–10μg/ml). Neither released IL-8 effectively alone, but each promoted IL-8 release with low-dose fMLF (1nM) (Fig. 3c). This is similar to GM-CSF priming of IL-8 release by CpG DNA. 22 These data suggest clinically significant activation of PMN secretion by mtDNA/TLR9. In distinction, TLR ligands have no direct effect on PMN chemotaxis (Supplementary Fig. 5).

To determine whether circulating mitochondrial DAMPs could cause neutrophil-mediated organ injury, we injected MTD equivalent to 5% of the rat’s liver intravenously and examined whether that recreated organ injury *in vivo*. Animals demonstrated marked inflammatory lung injury as early as 3h post-injection (Fig. 4a vs 4b). Oxidant lung injury was documented by staining for 4-hydroxy-2-nonenal (4-HNE) 24 (Fig. 4c vs 4d). MTD injection increased lung albumin (Fig. 4e) and wet/dry weight (Fig. 4f), IL-6 (Fig. 4g) as

well as elastase accumulation in lung (Supplementary Fig. 6). Bronchoalveolar lavage showed PMN influx into the airways (Fig. 4h), early appearance of TNF-α (Fig. 4i) and later appearance of IL-6 (Fig. 4j). PMN infiltration was confirmed as increased lung MMP-8 (Fig. 4k). Systemic inflammation was demonstrated as priming of circulating PMN (Fig. 1f) and their infiltration into liver (Fig. 4l). Control rats showed no evidence of pulmonary or hepatic inflammation.

In conclusion, inflammation occurs after both major trauma and infection16. Recognizing sterile SIRS is critical since empiric antimicrobial use will be ineffective whereas other therapies might be effective. After tissue trauma MTD circulates and stimulates PMN, causing systemic inflammation. The molecular similarity of mitochondria to their bacterial ancestors helps explain why traumatic and infective SIRS appear similar 3,25. Mitochondrial DAMPs express at least two molecular signatures (formyl peptides, mtDNA) that act on PRRs recognizing bacterial PAMPs. These activate PMN in the circulation (Figs. 1f, 2, 3) rather than at specific targets, inciting non-specific organ attack (Fig. 4) while suppressing chemotactic responsess to infective stimuli (Fig. 1c, 1e, and Supplementary Fig. 4).

Formyl peptides and mtDNA are likely only a subset of the DAMPs released by trauma, but they appear important at clinical concentrations. Other intracellular ‘alarmins’ may similarly be important after injury and other immune cells probably respond to mitochondrial DAMPs. Injury-derived mitochondrial DAMPs however, are clearly recognized by innate immunity using PRR that alternatively sense bacteria. This novel paradigm may explain why responses to ancient ‘enemies within’ released by injury can mimic sepsis.

Methods Summary

All studies were approved by the IRB of Beth Israel Deaconess Medical Center and Queen Mary University Hospital of London, England. Animal care was IACUC-approved per NIH guidelines.

Preparation of mitochondria, mitochondrial DAMPs (MTD) and mitochondrial DNA (mtDNA)

Mitochondria were isolated from resources per standard protocols.

PMN studies - general

PMN isolation 26, 27, calcium studies 15,16,26, Western blots 28, transwell chemotaxis 16, and video-microscopy chemotaxis assays 29 were performed as previously described.

MTD Administration

Male Sprague-Dawley rats were given intravenous MTD based on weight 30. qPCR of plasma showed mtDNA levels of 122±22 ng/ml 1h after injection (nl≪1ng/ml). Leukocytes in bronchoalveolar lavages were counted visually. Lungs were inflated gently and formalin fixed prior to stain with H&E or for 4-HNE.

Methods

Reagents and Chemicals

fMLF, ethyleneglycol-bis(β-aminoethylether)-N,N′-tetraacetic acid (EGTA), protease inhibitor cocktail and DMSO were purchased from Sigma (St Louis, MO). Fura-2 AM, Calcein AM and digitonin were purchased from Molecular Probes (Eugene, OR). Anti-human FPR1, anti-human FPRL-1, anti-human MMP-2, anti-human MMP-8, and anti-rat MMP-8 antibodies were purchased from R&D (Minneapolis, MN). Antibodies to phospho-p38 MAPK (Thr180/Tyr182), p38 MAPK, phospho-p44/42 MAPK (Thr202/Tyr204) and p44/42 MAPK were from Cell Signaling (Danvers, MA). Donkey anti-goat IgG-HRP was obtained from Santa Cruz (Santa Cruz, CA). ImmunoPure Goat Anti-Rabbit IgG (peroxidase conjugated) was purchased from Pierce Biotechnology (Rockford, IL). Cyclosporin H (CsH) was obtained from LKT Laboratories (St Paul, MN). ATP bioluminescence assay kits were purchased from Roche (Palo Alto, CA). W-peptide was from Phoenix pharmaceuticals (Burlingame, CA). CpG DNA was obtained from Cell Sciences (Canton, MA). ODN TTAGGG was purchased from InvivoGen (San Diego, CA).

Mitochondrial Isolation from Clinical Material

Clinical liver injury, muscle crush injury and femur fracture fixation by reamed nailing are all common, important events closely linked to inflammation and acute lung injury after injury. The Mitochondria Isolation Kit for Tissue (PIERCE, Rockford, IL) was used to isolate mitochondria from rat liver or rat muscle, human skeletal muscle (pathologic specimens amputated due to vascular disease); human femur medullary reamings from patients undergoing repair of femur fractures; and human liver from the margins of hepatic tumor resections. The Mitochondrial Isolation Kit for Cultured Cells (PIERCE, Rockford, IL) was used to isolate mitochondria from human rhabdomyosarcoma cells (ATCC, Manassas, VA). Clinical samples used to prepare mitochondria were harvested from patients receiving antibiotics. Mitochondria were isolated under sterile conditions at 4°C.

Preparation of Mitochondrial DAMPs (MTD) and mtDNA

Isolated mitochondrial pellets from tissue specimens (200mg) or rhabdomyosarcoma cells (6×10^7 cells) were suspended in 1ml of HBSS. Protease inhibitor cocktail (1:100) was added to the suspension. Since we found significant amounts of circulating mtDNA in trauma patients we surmised that mechanical tissue injury and/or tissue necrosis was disrupting mitochondria to some extent in vivo. So we standardized our experimental preparations with routine sonication on ice (VCX130-Vibra Cell, Sonics and Materials, Newtown, CT) at 100% amplitude (10X, 30s each time with 30s intervals). The disrupted mitochondrial suspensions were then centrifuged at 12,000 rpm for 10 min at 4°C followed by 100,000g at 4°C for 30min. Residual supernatants were used for experiments. Protein concentrations of the MTD solutions were determined by BCA assay (Pierce, Rockford, IL). mtDNA was extracted from the isolated mitochondria of various tissues using DNeasy Blood & Tissue kit (Qiagen, Valencia, CA). MTD and mtDNA were prepared under sterile conditions. Endotoxin levels were measured by limulus amebocyte lysate assay and did not achieve significant levels. mtDNA concentration was determined by spectrophotometer. No protein contamination was found and nuclear DNA was less than 0.01% by qPCR.

Real Time PCR protocols

Plasma DNA was prepared by QIAamp DNA Mini and Blood Mini kit (Qiagen, Valencia, CA). Primers for human cytochrome B (forward 5′-atgaccccaatacgcaaaat-3′ and reverse 5′-cgaagtttcatcatgcggag-3′), human cytochrome C oxidase subunit III (forward 5′-atgacccaccaatcacatgc -3′ and reverse 5′-atcacatggctaggccggag-3′), human NADH dehydrogenase (forward 5′-atacccatggccaacctcct-3′ and reverse 5′-gggcctttgcgtagttgtat-3′), rat cytochrome B (forward 5′-tccacttcatcctcccattc-3′ and reverse 5′-ctgcgtcggagtttaatcct-3′), rat cytochrome C oxidase subunit III (forward 5′-acataccaaggccaccaac-3′ and reverse 5′-cagaaaaatccggcaaagaa-3′), rat NADH dehydrogenase (forward 5′-caataccccaccccctttatc-3′ and reverse 5′-gaggctcatcccgatcatag-3′), and bacterial 16S ribosomal RNA (forward 5′-cgtcagctcgtgttgtgaaa-3′ and reverse 5′-ggcagtctccttgagttcc-3′) were synthesized by Invitrogen. Primer sequences have no significant homology with DNA found in any bacterial species published on BLAST. Real Time PCR standard curves were created to quantify mtDNA concentration by using purified mtDNA and Cytochrome B as targets. Samples that produced no PCR products after 40 cycles were considered “undetectable” and Ct set to 40 for statistical purposes.

PMN isolation

Detailed protocols are published elsewhere 26,27. Hypotonic lysis was performed on ice to remove contaminating RBC. This method results in preparations containing ≥98% neutrophils as confirmed by flow cytometry and confirmed visually on HEMA-3 stain with monocytes ~0.02% (Supplementary Fig. 7). Viability was ≥98% as assessed by Trypan Blue.

Chemotaxis assays by fluorescence videomicroscopy

Time-lapse video-microscopic chemotaxis was assayed as described previously 29. Cells were exposed to a chemoattractant gradient field by slowly releasing MTD (~100μg/ml) or fMLF (10nM) from a micropipette tip placed in proximity to the cells. The migration paths of individual cells were plotted using Adobe Illustrator. Cells were pretreated with or without 1μM CsH for 5min or 12.5μg/ml anti-human-FPR1 for 10min. Experiments were repeated with multiple PMN and MTD isolates. Specificity of CsH for FPR1 was examined in transwell chemotaxis assays. CsH significantly inhibited fMLF and MTD chemotaxis with no effects on IL-8.

In vivo chemotaxis

Male mice (8–10 wk, Charles River, Wilmington, MA) were used in this study. Mice were lightly anesthetized by isoflurane inhalation. CsH (10μM) or DMSO was injected intraperitoneally (i.p.). After 30min, 1ml of saline or W-peptide (10nM) or MTD (100μg/ml, equal to the mitochondria released by a 10% liver injury) was injected i.p.. Two hours later a peritoneal lavage was performed and collected for total and differential cell counts. Cell counts were performed on cytospin preparations stained with HEMA 3 (Fisher Scientific, Kalamazoo, MI).

PMN degranulation assays

PMN degranulation was assessed by measuring MMP-8 release. Human PMN were suspended in HBSS with 1.8mM Ca^{2+} at 37°C for 10min while exposed to MTD, mtDNA or fMLF at indicated concentrations. For inhibitor studies, PMN were pre-treated with CsH (10μM, 5min at 37°C), anti-FPR1 antibody (12.5μg/ml, 10min at 37°C or control antibodies as noted) or Inhibitory ODN TTAGGG (10/1 inhibitor to stimulus). After stimulation, PMN were placed on ice and centrifuged. Supernatants were then assayed for MMP-8 by Western blot. Residual PMN were lysed to assay for MAPKs.

ELISA

PMN were treated with various agonists for 4 hrs or 24 hrs. IL-8 was measured by human CXCL8/IL-8 ELISA (R&D, Minneapolis, MN). Experiments were performed in triplicate. TNF-α and IL-6 in rat BALF or lung were measured using BD OptEIA™ rat TNF and IL-6 ELISA sets (BD, San Diego, CA). Airway albumin was measured by rat albumin ELISA Quantitation kit (BETHYL, Montgomery, TX).

Statistical analysis

Study data was assessed for statistical significance using Student's (unpaired) *t*-test or Analysis of Variance (ANOVA) where appropriate using a SigmaStat program with post-hoc tests chosen by the computer. $[Ca^{2+}]_i$ transients are reported as the mean change from basal $[Ca^{2+}]_i$ in nanomoles per liter (nM). Prolonged $[Ca^{2+}]_i$ fluxes are reported as the area under the curve (AUC) of measured change from basal $[Ca^{2+}]_i$ over the observation period (nM·sec). All data are reported as mean ± s.e.m. with significance accepted at $p<0.05$.

Supplementary Material

Refer to Web version on PubMed Central for supplementary material.

Acknowledgments

This work is supported by National Institute of General Medical Sciences grant (C.J.H.) and DOD / CDMRP / DRMRP Hypothesis Development Award DR080924 (to C.J.H.).

References

1. Bone RC. Toward an epidemiology and natural history of SIRS (systemic inflammatory response syndrome). JAMA. 1992; 268:3452–5. [PubMed: 1460735]
2. Janeway CA Jr. Approaching the asymptote? Evolution and revolution in immunology. Cold Spring Harb Symp Quant Biol. 1989; 54(Pt 1):1–13. [PubMed: 2700931]
3. Matzinger P. Tolerance, danger, and the extended family. Annu Rev Immunol. 1994; 12:991–1045. [PubMed: 8011301]
4. Sagan L. On the origin of mitosing cells. J Theor Biol. 1967; 14:255–74. [PubMed: 11541392]
5. Sasser SM, et al. Guidelines for field triage of injured patients. Recommendations of the National Expert Panel on Field Triage. MMWR Recomm Rep. 2009; 58:1–35. [PubMed: 19165138]
6. Abraham E. Neutrophils and acute lung injury. Crit Care Med. 2003; 31:S195–9. [PubMed: 12682440]
7. Fine J, Frank ED, Ravin HA, Rutenberg SH, Schweinburg FB. The bacterial factor in traumatic shock. N Engl J Med. 1959; 260:214–20. [PubMed: 13622952]

8. Moore FA, et al. Gut bacterial translocation via the portal vein: a clinical perspective with major torso trauma. J Trauma. 1991; 31:629–36. discussion 636–8. [PubMed: 2030509]
9. Deitch EA, Xu D, Kaise VL. Role of the gut in the development of injury- and shock induced SIRS and MODS: the gut-lymph hypothesis, a review. Front Biosci. 2006; 11:520–8. [PubMed: 16146750]
10. Marcker K, Sanger F. N-Formyl-Methionyl-S-Rna. J Mol Biol. 1964; 8:835–40. [PubMed: 14187409]
11. Taanman JW. The mitochondrial genome: structure, transcription, translation and replication. Biochim Biophys Acta. 1999; 1410:103–23. [PubMed: 10076021]
12. Baker SP, O'Neill B, Haddon W Jr, Long WB. The injury severity score: a method for describing patients with multiple injuries and evaluating emergency care. J Trauma. 1974; 14:187–96. [PubMed: 4814394]
13. Schiffmann E, Corcoran BA, Wahl SM. N-formylmethionyl peptides as chemoattractants for leucocytes. Proc Natl Acad Sci U S A. 1975; 72:1059–62. [PubMed: 1093163]
14. Rabiet MJ, Huet E, Boulay F. Human mitochondria-derived N-formylated peptides are novel agonists equally active on FPR and FPRL1, while Listeria monocytogenes-derived peptides preferentially activate FPR. Eur J Immunol. 2005; 35:2486–95. [PubMed: 16025565]
15. Hauser CJ, et al. Major trauma enhances store-operated calcium influx in human neutrophils. J Trauma. 2000; 48:592–7. discussion 597–8. [PubMed: 10780589]
16. Tarlowe MH, et al. Inflammatory chemoreceptor cross-talk suppresses leukotriene B4 receptor 1-mediated neutrophil calcium mobilization and chemotaxis after trauma. J Immunol. 2003; 171:2066–73. [PubMed: 12902512]
17. West MA, et al. Whole blood leukocyte mitogen activated protein kinases activation differentiates intensive care unit patients with systemic inflammatory response syndrome and sepsis. J Trauma. 2007; 62:805–11. [PubMed: 17426533]
18. Wenzel-Seifert K, Seifert R. Cyclosporin H is a potent and selective formyl peptide receptor antagonist. Comparison with N-t-butoxycarbonyl-L-phenylalanyl-L-leucyl-L-phenylalanyl-L-leucyl-L-phenylalanine and cyclosporins A, B, C, D, and E. J Immunol. 1993; 150:4591–9. [PubMed: 8387097]
19. Van Lint P, Libert C. Matrix metalloproteinase-8: cleavage can be decisive. Cytokine Growth Factor Rev. 2006; 17:217–23. [PubMed: 16820317]
20. Cardon LR, Burge C, Clayton DA, Karlin S. Pervasive CpG suppression in animal mitochondrial genomes. Proc Natl Acad Sci U S A. 1994; 91:3799–803. [PubMed: 8170990]
21. Collins LV, Hajizadeh S, Holme E, Jonsson IM, Tarkowski A. Endogenously oxidized mitochondrial DNA induces in vivo and in vitro inflammatory responses. J Leukoc Biol. 2004; 75:995–1000. [PubMed: 14982943]
22. Hayashi F, Means TK, Luster AD. Toll-like receptors stimulate human neutrophil function. Blood. 2003; 102:2660–2669. [PubMed: 12829592]
23. Lee SH, Lee JG, Kim JR, Baek SH. Toll-like receptor 9-mediated cytosolic phospholipase A2 activation regulates expression of inducible nitric oxide synthase. Biochem Biophys Res Commun. 2007; 364:996–1001. [PubMed: 18273445]
24. Uchida K, Szweda LI, Chae HZ, Stadtman ER. Immunochemical detection of 4-hydroxynonenal protein adducts in oxidized hepatocytes. Proc Natl Acad Sci U S A. 1993; 90:8742–6. [PubMed: 8378358]
25. Seong SY, Matzinger P. Hydrophobicity: an ancient damage-associated molecular pattern that initiates innate immune responses. Nat Rev Immunol. 2004; 4:469–78. [PubMed: 15173835]
26. Hauser CJ, et al. PAF-mediated Ca2+ influx in human neutrophils occurs via store-operated mechanisms. J Leukoc Biol. 2001; 69:63–8. [PubMed: 11200069]
27. Fekete Z, et al. Injury-enhanced calcium mobilization in circulating rat neutrophils models human PMN responses. Shock. 2001; 16:15–20. [PubMed: 11442309]
28. Zhang Q, et al. Molecular mechanism(s) of burn-induced insulin resistance in murine skeletal muscle: role of IRS phosphorylation. Life Sci. 2005; 77:3068–77. [PubMed: 15982669]
29. Chen Y, et al. ATP release guides neutrophil chemotaxis via P2Y2 and A3 receptors. Science. 2006; 314:1792–5. [PubMed: 17170310]

30. Hauser CJ. Preclinical models of traumatic, hemorrhagic shock. Shock. 2005; 24 (Suppl 1):24–32. [PubMed: 16374369]

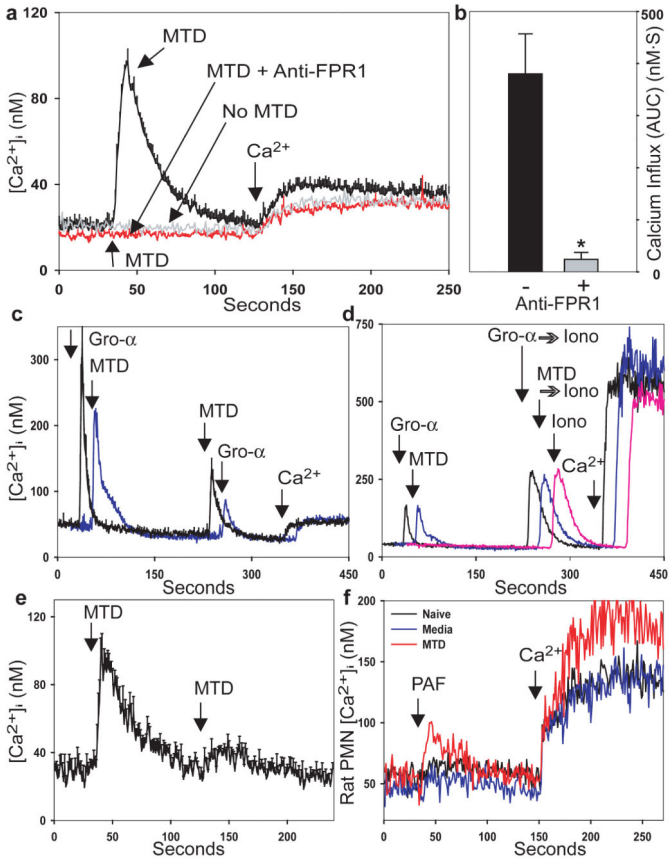

FIGURE 1. PMN $[Ca^{2+}]_i$ responses to MTD

Rhabdomyosarcoma-derived125125 MTD (1.2μg/ml protein) induces Ca^{2+} store depletion (**a**) and Ca^{2+} influx (**a, b**) in human PMN. (*p=0.01, *t*-test). **c,** PMN serially exposed to MTD and GRO-α (CXCL1) exhibit heterologous desensitization. **d,** PMN stimulated with GRO-α or MTD show equal store release by ionomycin. **e**, PMN show homologous desensitization of $[Ca^{2+}]_i$ responses to MTD. **f**, Systemic injection of MTD increases rat PMN responses to PAF. Traces with error bars are from ≥3 experiments, other traces are exemplary. Traces may be displaced temporally for clarity.

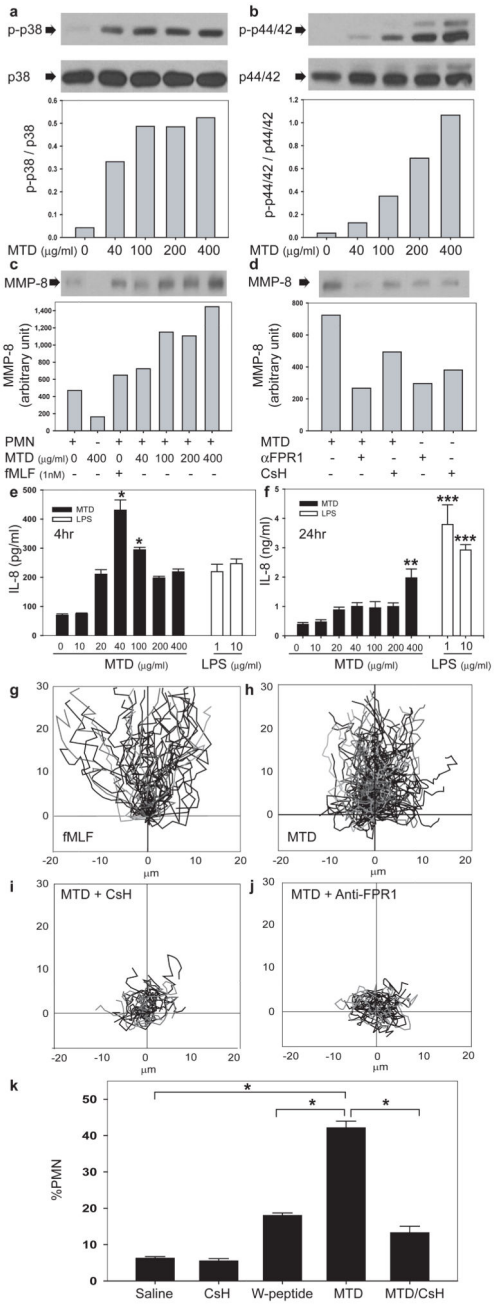

FIGURE 2. MTD activate PMN

Human PMN exposed to human MTD (muscle) were immunoblotted for phosphorylated and total (control) p38 (**a**) or p44/42 MAPK (**b**). MMP-8 was immunoblotted in supernatants (**c**,**d** are from same gel). αFPR1 denotes anti-FPR1. **e–f,** MTD elicits PMN IL-8 synthesis: */** denote $p<0.05$ versus control. *** denotes $p<0.05$ (ANOVA/Tukey) versus control or MTD (n=3). PMN chemotaxis to fMLF and MTD was analyzed by video-microscopy (g,h, Videos 1,2). CsH or anti-FPR1 drastically inhibit chemotaxis (i,j, Videos 3,4). MTD injection into the mouse peritoneum (**k**) causes rapid, CsH-inhibitable neutrophil influx (n=6, *$p<0.05$, ANOVA/Dunn) compared with saline or 10nM W-peptide controls.

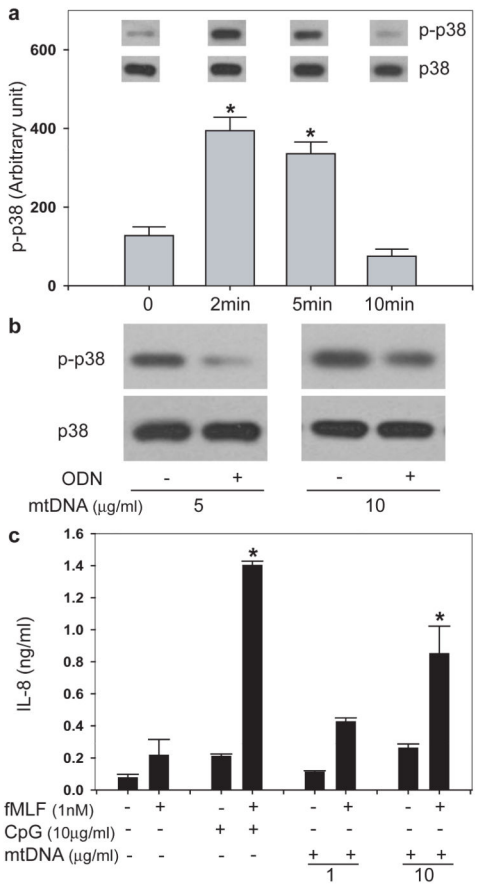

FIGURE 3. mtDNA activates PMN via CpG/TLR9 interactions

a, Incubation of PMN (10^6) with 1μg/ml mtDNA activates p38 MAPK (n=3, *p<0.05 vs unstimulated cells). **b**, mtDNA-induced activation of p38 MAPK was inhibited by pre-treatment with the inhibitory ODN TTAGGG. Inhibition was overcome at higher mtDNA concentration. **c,** PMN were co-incubated in 1nM fMLF plus mtDNA at clinical concentrations (1–10μg/ml, see Supplementary Fig. 1d). Neither CpG-DNA nor mtDNA caused IL-8 release alone, but each caused significant release along with low dose fMLF. (n=3, *p< 0.05 compared with unstimulated control) (all tests ANOVA/Dunn).

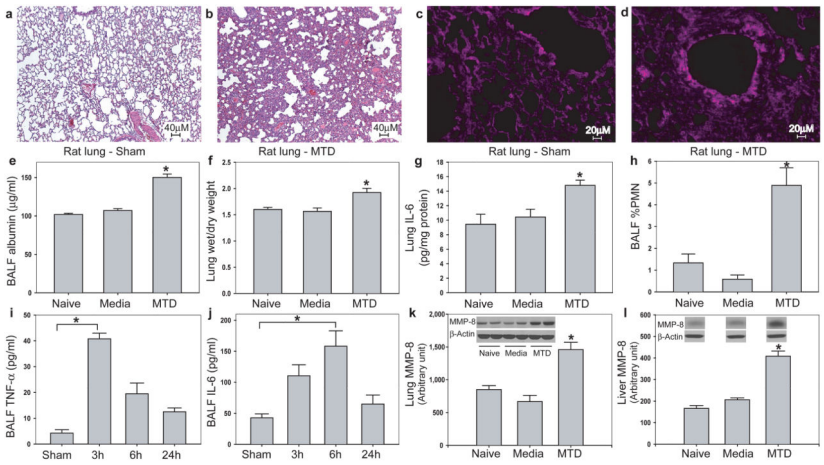

FIGURE 4. MTD cause systemic inflammation and organ injury *in vivo*

Rats given intravenous MTD equivalent to mitochondria from a 5% liver injury show marked evidence of lung injury by H&E histology **(a–b)** and 4-HNE stain for oxidant injury (**c–d**). MTD increased pulmonary albumin permeability (**e**), lung wet/dry weight (**f**), accumulation of IL-6 in lung (**g**) and PMN infiltration into the airways (**h**). Early (3h) appearance of TNF-α (**i**) and late (6h) appearance of IL-6 (**j**) were noted in lung lavage fluid. Whole lung (**k**) and liver (**l**) MMP-8 confirmed increased PMN infiltration. (all studies n≥3, *p<0.05, ANOVA/post-hoc).